Article

Discovery Medicine 2025; 37(201): 2256–2268
https://doi.org/10.24976/Discov.Med.202537201.192

TRPML1 Modulates Calcium Signaling to Coordinate Mitochondria–Lysosome Crosstalk in Spinal Cord Injury Repair

Jinglong Zhang[1,†], Jing Kong[2,†], Zhiyong Zhao[1], He Zhang[1], Ruobing Bai[1], Shuai Yuan[1,*]

[1]Department of Neurosurgery, Lanzhou University Second Hospital, 730030 Lanzhou, Gansu, China
[2]Department of Health Management Center, Lanzhou University Second Hospital, 730030 Lanzhou, Gansu, China
*Correspondence: yuanshuai0611@163.com (Shuai Yuan)
[†]These authors contributed equally.
Submitted: 9 July 2025 Revised: 19 August 2025 Accepted: 29 August 2025 Published: 20 October 2025

Background: Spinal cord injury (SCI) results in profound neurological dysfunction, involving calcium dysregulation, mitochondrial impairment, and lysosomal dysfunction. Transient receptor potential mucolipin 1 (TRPML1), a lysosomal calcium-permeable channel, plays a pivotal role in cellular homeostasis and lysosome–mitochondria crosstalk. Therefore, this study aims to elucidate the functional role and regulatory mechanisms of TRPML1 in SCI repair.

Methods: A T9–T10 contusive SCI model was established in C57BL/6 mice. TRPML1 was overexpressed via adeno-associated virus (AAV9), and its effects were assessed through behavioral assessments, histopathological examination, and molecular analyses. Furthermore, a hydrogen peroxide (H_2O_2)-induced NSC-34 motor neuron-like cell injury model was employed to validate the mechanisms *in vitro*.

Results: *In vivo*, TRPML1 overexpression significantly enhanced the expression of mitochondrial and lysosomal functional proteins (transcription factor EB [TFEB], lysosomal-associated membrane protein 1 [LAMP1], ATP synthase-α 1 [ATP5A1]), suppressed Cytochrome C levels, restored mitochondrial membrane potential, and alleviated both calcium overload and reactive oxygen species (ROS) accumulation ($p < 0.01$). Furthermore, terminal deoxynucleotidyl transferase dUTP nick end labeling (TUNEL) staining revealed decreased apoptosis, whereas histological analysis showed preserved spinal cord architecture and diminished inflammatory infiltration. Additionally, basso mouse scale (BMS) scores demonstrated improved locomotor recovery. *In vitro*, TRPML1 was found to alleviate H_2O_2-induced NSC-34 cell damage, as evidenced by restored calcium homeostasis, reduced ROS, enhanced mitochondrial function, and attenuated apoptosis, indicating its consistent neuroprotective effects across models.

Conclusion: TRPML1 exerts neuroprotective effects by modulating calcium signaling and coordinating mitochondrial and lysosomal function, highlighting its therapeutic potential as a promising target for managing SCI repair.

Keywords: TRPML1; spinal cord injury; calcium signaling; mitochondrial homeostasis; lysosome–mitochondria crosstalk; oxidative stress

Introduction

Spinal cord injury (SCI) is a devastating central nervous system disease characterized by disrupted calcium homeostasis, mitochondrial dysfunction, and lysosomal impairment [1–3]. Globally, over 20 million individuals are living with SCI, with approximately 0.9 million new cases each year, leading to significant health challenges due to premature mortality and long-term disability [4]. Current treatment approaches primarily focus on addressing secondary injury cascades and functional rehabilitation through interventions such as functional electrical stimulation and partial-weight-supported walking [5]. However, these interventions offer only limited neurological restoration function, underscoring the urgent need for novel therapeutic strategies that target critical molecular pathways.

Following the initial mechanical trauma, SCI triggers a cascade of molecular events, including glutamate-mediated excitotoxicity, excessive calcium influx with subsequent free radical production, and oligodendrocyte apoptosis, all of which collectively exacerbate neuronal damage [5]. These secondary injury cascades progressively disrupt mitochondria-lysosome interactions, leading to metabolic imbalance and progressive neuronal degeneration [6,7]. Recent evidence shows that the transient receptor potential mucolipin 1 (TRPML1), a calcium-permeable channel located on the lysosomal membrane, plays a crucial role in regulating mitochondria–lysosome crosstalk and maintaining neuronal homeostasis, with its dysfunction closely linked to SCI pathology [8,9].

Calcium signaling is essential for regulating mitochondrial and lysosomal function following SCI. Mitochondria rely on calcium fluxes to drive adenosine triphosphate (ATP) synthesis, support oxidative phosphorylation, and modulate autophagy [10,11]. However, SCI often leads to calcium overload, which induces mitochondrial damage and increases oxidative stress [12]. Simultaneously, lysosomal degradation capacity is compromised, hindering the clearance of damaged organelles and aggravating neuronal injury [13]. This calcium dysregulation establishes a vicious feedback loop—excessive Ca^{2+} influx through damaged membranes activates caspase-3-mediated apoptosis [14], while lysosomal dysfunction promotes the accumulation of dysfunctional mitochondria, further exacerbating oxidative stress [15]. Importantly, the Annexin A7 (ANXA7)–Peroxisome Proliferator-Activated Receptor Gamma (PPARγ) axis reveals the role of lipid droplet-mitochondria interactions modulating calcium homeostasis [16], and zebrafish models show that gap junction-mediated calcium buffering can promote neuronal survival [17], offering potential therapeutic insights for axonal regeneration.

TRPML1 plays a crucial role in maintaining neuronal balance by promoting lysosomal biogenesis via the transcription factor EB (TFEB) signaling pathway and sustaining mitochondria–lysosome communication via lysosomal-associated membrane protein 1 (LAMP1), thereby regulating cellular energy metabolism and autophagy [8,18]. Activation of TRPML1 has been reported to alleviate calcium dysregulation, restore mitochondrial function, and enhance neuronal survival following SCI [19]. Oxidative stress is substantially increased post-SCI, as evidenced by higher mitochondrial reactive oxygen species (ROS) production and impaired antioxidant defense mechanisms [20]. TRPML1 activation mitigates ROS accumulation by promoting the clearance of damaged mitochondria via the TFEB-mediated pathway, thereby reducing oxidative stress [21]. Furthermore, TRPML1 helps stabilize the mitochondrial membrane potential ($\Delta\Psi m$), enhances the efficiency of ATP synthesis, and supports neuronal viability by modulating lysosomal calcium signaling [22].

Neuronal apoptosis post-SCI is primarily mediated by the crosstalk between mitochondria and lysosomes. Lysosomal rupture releases proteases such as cathepsin B, which activate mitochondrial apoptotic pathways [23]. TRPML1 has been shown to counteract this process by promoting autophagy through the AMP-activated protein kinase (AMPK)–TRPML1–Calcineurin axis, thereby suppressing the expression of pro-apoptotic proteins and reducing neuronal death [24]. Notably, the downregulation of TRPML1 following SCI has enhanced the investigation of therapeutic strategies such as adeno-associated virus (AAV)-mediated TRPML1 overexpression and the application of TRPML1 agonists [25,26]. These approaches have demonstrated promising outcomes in restoring mitochondria–lysosome calcium communication and improving neuronal survival [27]. Furthermore, *in vitro* studies, such as those by Sapienza *et al*. [28], suggest a regulatory role of TRPML1 in maintaining calcium dynamics and mitochondrial–lysosomal integrity under oxidative stress in NSC-34 motor neurons. However, the precise mechanisms by which TRPML1 coordinates calcium signaling and organelle function within the complex pathophysiology of SCI remain to be fully explored.

Therefore, this study aims to elucidate the role and underlying mechanisms of TRPML1 in SCI repair, with a particular focus on its involvement in calcium signaling regulation, mitochondria–lysosome interactions, and apoptosis inhibition. Unraveling these mechanisms may provide novel and valuable insights into SCI pathogenesis and identify potential therapeutic targets for improved treatment approaches.

Materials and Methods

Experimental Animals

Initially, male C57BL/6 mice (8–12 weeks old, weighing 18–25 g) obtained from the Guangdong Provincial Medical Laboratory Animal Center (Guangzhou, China). All animals were acclimated for one week under controlled environmental conditions (22 $\pm$ 2 °C, 50–60% humidity, and a 12-hour light/dark cycle) with free access to food and water. All animal protocols and experimental designs were approved by the Animal Ethics Committee of the Guangdong Provincial Medical Laboratory Animal Center, China (Approval No. D202504-11) and conducted in accordance with institutional and national guidelines for animal research.

SCI Modeling and Experimental Grouping

A contusive SCI model at the T9–T10 level was established using a modified Allen's method [29]. Mice were anesthetized via intraperitoneal injection of sodium pentobarbital (50 mg/kg, 1% w/v solution; #P3761, Sigma-Aldrich, St. Louis, MO, USA), and anesthesia depth was verified by the absence of toe-pinch reflex. Once fully anesthetized, a dorsal laminectomy was performed to expose the spinal cord, followed by a calibrated contusion using a standardized impactor (10 g $\times$ 2.5 cm; IH-0400, Precision Systems and Instrumentation, Lexington, KY, USA). Sham-operated control mice underwent a laminectomy without spinal cord impact. All animals received postoperative ceftriaxone (25 mg/kg/day, i.p.; #HY-B0712, MedChemExpress, Monmouth Junction, NJ, USA) for three days and were maintained at 37 °C until full recovery.

To assess the functional role of TRPML1 in SCI repair, recombinant AAV9 vectors (Addgene, #107790, Watertown, MA, USA) were employed to deliver either full-length murine TRPML1 cDNA or an empty vector control. TRPML1 expression was driven by the Calcium/Calmodulin-Dependent Protein Kinase II Alpha

(CamKIIα) promoter, enabling preferential expression in excitatory neurons, though minimal expression in non-neuronal cells could not be excluded. The overexpression cassette was based on the pcDNA3.1 backbone which contains a cytomegalovirus enhancer, a woodchuck hepatitis virus post-transcriptional regulatory element (WPRE), and a bovine growth hormone polyadenylation signal. The empty (control) vector in the SCI + Oe-NC group retained the same backbone structure but lacked the TRPML1 insert. Both vector constructs harbored an ampicillin resistance gene for bacterial selection. The complete nucleotide sequence of the TRPML1 overexpression construct is provided in **Supplementary Table 1**.

Immediately following SCI induction (within 30 minutes), a 2 µL of AAV9 viral suspension (1×10^{12} vg/mL) was bilaterally microinjected into the spinal cord parenchyma at the injury epicenter (0.5 µL/min) using a Hamilton microsyringe (Model 84250, Hamilton Company, Reno, NV, USA) fitted with a pulled-glass capillary. To minimize reflux, the needle was held in place for an additional 10 minutes before slow retraction was initiated. To account for the ~14-day delay in AAV-mediated gene expression, behavioral assessments were extended to 28 days post-injury to ensure that all phenotypic evaluations were performed after confirmed transgene overexpression.

Animals were randomly assigned into four experimental groups (n = 12 per group): (a) Sham group (laminectomy only, without SCI, serving as the control) [19]; (b) SCI group (SCI model without any genetic manipulation); (c) SCI + Oe-NC group (SCI + AAV9 carrying an empty pcDNA3.1 vector); (d) SCI + Oe-TRPML1 group (SCI + AAV9 carrying the TRPML1 overexpression vector). At designated timepoints, mice were re-anesthetized using the same protocol and euthanized by cervical dislocation under deep anesthesia. Spinal cord segments (5 mm) surrounding the injury epicenter were then harvested for subsequent molecular, histological, or biochemical analyses.

Motor Function Assessment

Motor function recovery was evaluated using the basso mouse scale (BMS) on days 1, 3, 7, 14, 21, and 28 post-injuries [30]. The BMS is a 9-point scale (0–8) designed to assess hindlimb locomotor function in open-field tests, focusing on joint movement, weight support, coordination, and paw positioning. Each mouse was placed in a circular arena (115 cm diameter) and observed for 4 minutes by two trained evaluators who were blinded to the group allocation. To minimize subjective bias, evaluators underwent standardized training, including video-based calibration and consensus scoring with expert raters, which achieved an inter-rater reliability of >0.90. Final BMS scores were calculated as the average of the two independent assessments, and hindlimb locomotor scores were recorded to assess functional outcomes.

Hematoxylin and Eosin (H&E) Staining of SCI Tissues

Fixed SCI tissue samples were dehydrated, cleared, and embedded in paraffin. These paraffin-embedded tissues were sectioned into 4–6 µm thick slices, baked at 60 °C for 30 minutes, dewaxed in xylene, and rehydrated through an ethanol gradient. After rinsing with distilled water, the sections underwent H&E staining, followed by dehydration and mounting with neutral resin. The prepared slides were then visualized and imaged under a light microscope (Olympus BX53, Tokyo, Japan).

Cell Culture and Experimental Grouping

NSC-34 mouse motor neuron-like cells (#HTX1846, Huatuo Biotech, Shenzhen, China) were cultured in high-glucose Dulbecco's Modified Eagle Medium (DMEM; #11965092, Thermo Fisher Scientific, Waltham, MA, USA) supplemented with 10% fetal bovine serum (FBS) and 1% penicillin–streptomycin and incubated at 37 °C in the presence of 5% CO_2. Short tandem repeat (STR) authentication was performed by the supplier to confirm the identity of the NSC-34 cell line. All cells were confirmed to be mycoplasma-free using polymerase chain reaction (PCR)-based testing (MycoAlert™, Lonza, Walkersville, MD, USA) before experiments and were monitored monthly thereafter. Cells at passages 3–5 were used for subsequent experiments. To mimic the oxidative stress microenvironment observed after SCI, cells were treated with 400 µM hydrogen peroxide (H_2O_2) for 24 hours [31]. Based on experimental design, cells were subjected to H_2O_2 treatment alone or in combination with transfection using either an empty vector (pcDNA3.1) or a TRPML1-overexpressing plasmid (pcDNA3.1-TRPML1). This yielded four groups: Control, H_2O_2, H_2O_2 + Oe-NC, and H_2O_2 + Oe-TRPML1. Transfections were performed using Lipofectamine 3000 (#L3000150, Invitrogen, Thermo Fisher Scientific, Waltham, MA, USA) according to the manufacturer's instructions, and all assays were conducted 48 hours post-transfection.

qRT-PCR Analysis

Total RNA was extracted from SCI tissues and NSC-34 cells using TRIzol reagent (#15596018CN, Invitrogen, Thermo Fisher Scientific, Waltham, MA, USA), and subsequently reverse-transcribed using a cDNA synthesis kit (#6210A, Takara, Shiga, Japan). Quantitative real-time polymerase chain reaction (qRT-PCR) was conducted using sensitive fluorescent DNA binding stain (SYBR) Green qPCR Master Mix (#639676, Takara, Shiga, Japan) on an ABI 7500 Real-Time PCR System (Applied Biosystems, Thermo Fisher Scientific, Foster City, CA, USA), with glyceraldehyde 3-phosphate dehydrogenase (GAPDH) serving as an internal control. Relative gene expression was determined using the $2^{-\Delta\Delta Ct}$ method, and each experiment was performed. The primer se-

quences used in qRT-PCR were as follows: TRPML1-F: 5′-CAAGACCCACATCCAGGAGT-3′, TRPML1-R: 5′-ACAAACTCGTTCTGCAGCAG-3′; GAPDH-F: 5′-AGTATGACTCCACTCACGGC-3′, GAPDH-R: 5′-CACCAGTAGACTCCACGACA-3′.

TUNEL Assay

Apoptosis in SCI tissues and NSC-34 cells was evaluated using a terminal deoxynucleotidyl transferase dUTP nick end labeling (TUNEL) assay kit (#C1088, Beyotime, Shanghai, China). Samples were fixed with 4% paraformaldehyde (#P1110, Solarbio, Beijing, China) for 30 minutes, permeabilized with 0.3% Triton X-100 (#ST795, Beyotime, Shanghai, China), and incubated with the TUNEL reaction solution at 37 °C for 1 hour in the dark. Nuclei were counterstained with 4′6-diamidino-2-phenylindole (DAPI; #C1002, Beyotime, Shanghai, China) for 10 minutes. Fluorescent images were acquired using a fluorescence microscope (IX73, Olympus, Tokyo, Japan), and the apoptotic index was calculated as the percentage of TUNEL-positive cells in five randomly selected fields using ImageJ software (version 1.53, NIH, Bethesda, MD, USA).

Kit-Based Detection Assays

Total calcium levels in spinal cord tissues were measured using a calcium colorimetric assay kit (#S1063S, Beyotime, Shanghai, China). Briefly, fresh tissues were homogenized in lysis buffer and centrifuged at 12,000 ×g for 10 minutes at 4 °C, and the resulting supernatants were then mixed with detection reagents (1:1 buffer/color reagent). Absorbance was recorded at 575 nm using a fluorescence microplate reader (Varioskan™ LUX, Thermo Fisher Scientific, Waltham, MA, USA), and concentrations were calculated using a 0–1.0 mM calcium standard curve.

Intracellular Ca^{2+} dynamics in NSC-34 cells were assessed using Fluo-4 AM (#S1060, Beyotime, Shanghai, China). After H_2O_2 treatment and washing, cells were incubated with the dye for 30 minutes at 37 °C, followed by a 20-minute incubation in dye-free medium for de-esterification. Fluorescence intensity was determined at 494 nm excitation and 516 nm emission using a fluorescence microplate reader (Varioskan™ LUX, Thermo Fisher Scientific, Waltham, MA, USA). Background values were corrected, and findings were expressed as relative fluorescence units (RFU).

Reactive oxygen species (ROS) levels were detected using the DCFH-DA probe (#S0034, Beyotime, Shanghai, China). For tissue samples, fluorescence intensity was recorded using a fluorescence microplate reader at 488 nm excitation and 525 nm emission to reduce background interference during imaging. For cell samples, fluorescence images were acquired under a fluorescence microscope (Olympus BX53, Tokyo, Japan).

$\Delta\Psi$m was evaluated using the JC-1 assay kit (#C2006, Beyotime, Shanghai, China). For tissue samples, homogenates were incubated with a JC-1 working solution (5×10^5 cells/mL) for 15–30 minutes at 37 °C. Red fluorescence (JC-1 aggregates, Ex/Em: 585/590 nm) and green fluorescence (monomers, Ex/Em: 514/529 nm) were measured using a fluorescence microplate reader, and the red-to-green fluorescence ratio was calculated to assess $\Delta\Psi$m. For cultured cells, JC-1 staining was performed under the same conditions, and $\Delta\Psi$m was determined using fluorescence microscopy.

Mitochondrial ROS levels in tissue samples were evaluated using MitoSOX Red (#M36008, Thermo Fisher Scientific, Waltham, MA, USA). Tissues were incubated with 5 µM MitoSOX Red for 10 minutes at 37 °C, washed, and fluorescence was recorded at an excitation of 510 nm and an emission of 610 nm using a fluorescence microplate reader. Data were normalized to protein content and corrected for background fluorescence.

Western Blotting

SCI tissues and NSC-34 cells from different experimental groups were lysed using radio immunoprecipitation assay (RIPA) lysis buffer (Beyotime, Shanghai, China), sonicated, and centrifuged at 12,000 rpm for 15 minutes at 4 °C. Protein concentrations were determined using a bicinchoninic acid (BCA) protein assay kit (Beyotime, Shanghai, China), and equal protein amounts (30 µg) were resolved on a 10% sodium dodecyl sulfate-polyacrylamide gel electrophoresis (SDS-PAGE) gel and then transferred onto a polyvinylidene fluoride (PVDF) membrane (Millipore, Burlington, MA, USA). The membranes were blocked with 5% skim milk for 1 hour, and incubated overnight at 4 °C with the following primary antibodies (1:1000): TRPML1 (PA1-46474, Thermo Fisher Scientific, Waltham, MA, USA), TFEB (ab267351, Abcam), LAMP1 (ab24170, Abcam), ATP synthase-α 1 (ATP5A1; ab14748, Abcam), Cytochrome C (ab133504, Abcam), calmodulin (CALM; ab45689, Abcam), and mitochondrial calcium uniporter (MCU; ab121499, Abcam). β-Actin (1:5000, ab8227, Abcam) was used as the internal control. The following day, the membranes were washed and incubated with horseradish peroxidase (HRP)-conjugated secondary antibodies (anti-mouse IgG-HRP, ab205719; anti-rabbit IgG-HRP, ab6721; 1:5000, Abcam) for 1 hour at room temperature. Finally, protein bands were visualized using an enhanced chemiluminescence (ECL) detection kit (#32106, Thermo Fisher Scientific, Waltham, MA, USA) and quantified with ImageJ, with β-actin serving as an internal reference.

Statistical Analysis

Statistical analyses were conducted using SPSS 26.0 software (IBM Corp., Armonk, NY, USA). Differences between the two groups were assessed using unpaired *t*-tests,

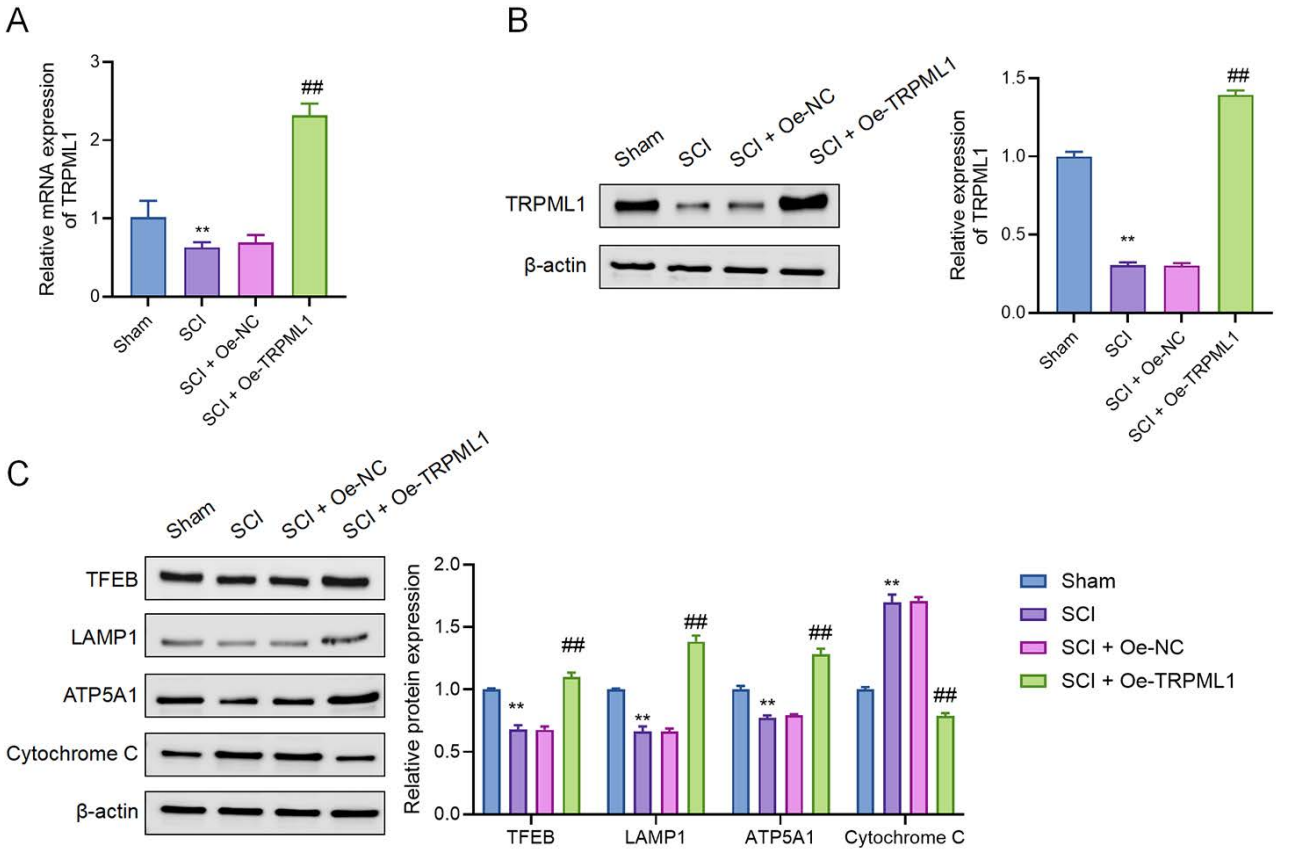

Fig. 1. TRPML1 overexpression restores its expression and improves lysosomal and mitochondrial function after SCI. (A) qRT-PCR analysis of TRPML1 mRNA expression in spinal cord tissues across different groups (n = 12). (B) Western blot analysis and quantitative results of TRPML1 protein expression. (C) Western blot analysis and quantification of lysosomal proteins (TFEB, LAMP1) and mitochondrial proteins (ATP5A1, Cytochrome C). Data are expressed as mean ± SD (n = 3). ** $p < 0.01$ vs. Sham group; $^{\#\#}$ $p < 0.01$ vs. SCI + Oe-NC group. TRPML1, transient receptor potential mucolipin 1; SCI, spinal cord injury; TFEB, transcription factor EB; LAMP1, lysosomal-associated membrane protein 1; qRT-PCR, quantitative real-time polymerase chain reaction; SD, standard deviation; ATP5A1, ATP synthase-α 1.

and multiple group comparisons were conducted via one-way ANOVA followed by Tukey's post hoc test. Results were expressed as mean ± standard deviation (SD), and a p-value of <0.05 was considered statistically significant.

Results

TRPML1 Overexpression Reverses SCI-Induced Lysosomal and Mitochondrial Function

To investigate the role of TRPML1 in SCI repair, its expression in spinal cord tissues was examined using qRT-PCR and western blot analysis. As shown in Fig. 1A,B, TRPML1 mRNA and protein levels were significantly reduced in the SCI group compared to the Sham group but were robustly restored in the SCI + Oe-TRPML1 group, exceeding even Sham levels ($p < 0.01$). These findings indicate that SCI suppresses endogenous TRPML1 expression, which can be effectively rescued by AAV-mediated overexpression of TRPML1.

Furthermore, we examined the impact of TRPML1 overexpression on organelle function. As shown in Fig. 1C, expression levels of the lysosomal markers TFEB and LAMP1, and the mitochondrial marker ATP5A1, were significantly reduced after SCI, while Cytochrome C levels were elevated, suggesting organelle dysfunction. However, TRPML1 overexpression reversed these alterations, restoring TFEB, LAMP1, and ATP5A1 levels, and reducing Cytochrome C expression ($p < 0.01$), thereby supporting its role in maintaining lysosomal and mitochondrial homeostasis following SCI.

TRPML1 Overexpression Restores Calcium Homeostasis and Mitochondrial Function After SCI

To further explore the role of TRPML1 in calcium regulation and mitochondrial integrity, western blot analysis was performed for CALM and MCU. As shown in Fig. 2A, both proteins were downregulated after SCI, whereas their expression was substantially restored in the SCI + Oe-

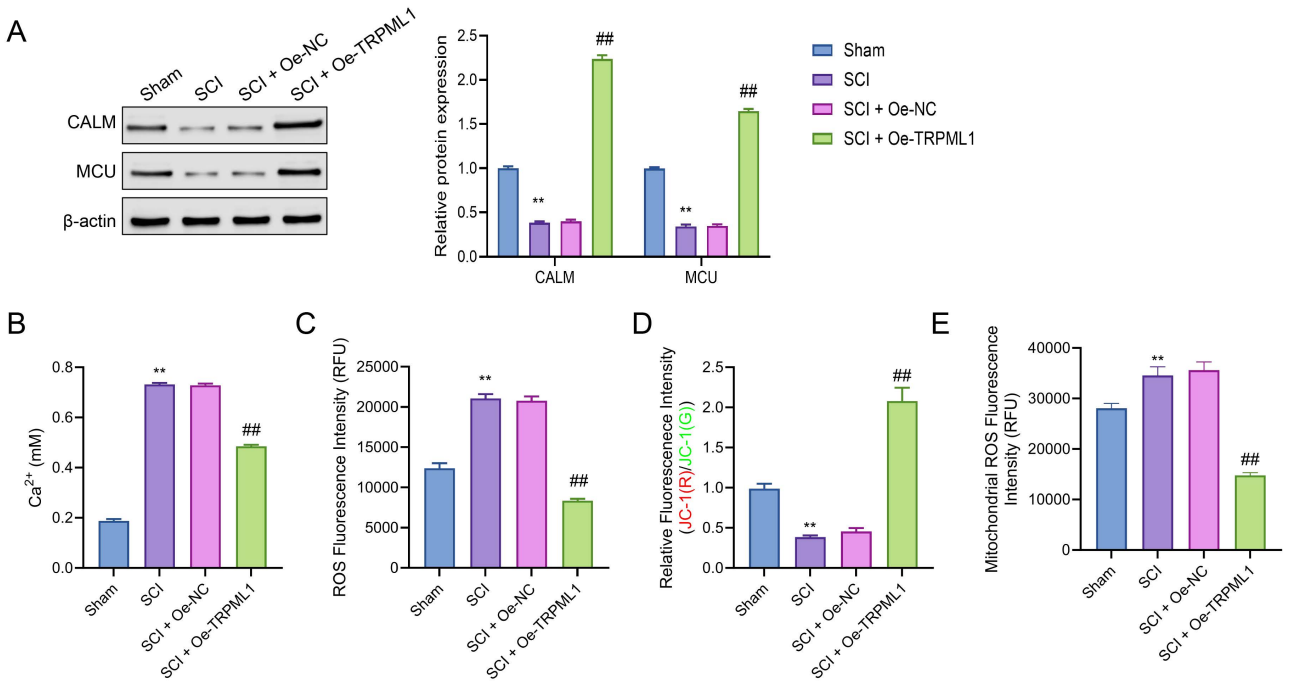

Fig. 2. TRPML1 overexpression restores calcium homeostasis and mitochondrial function following SCI. (A) Western blot analysis and quantification of CALM and MCU protein expression in spinal cord tissues (n = 3). (B) Total calcium levels were assessed using a calcium assay kit. (C) Intracellular ROS levels were detected using DCFH-DA fluorescence. (D) JC-1 staining for mitochondrial membrane potential (ΔΨm). Red fluorescence (JC-1[R]) indicates high ΔΨm, whereas green fluorescence (JC-1[G]) indicates low ΔΨm. The relative ΔΨm was expressed as red-to-green fluorescence ratio. (E) MitoSOX assay for mitochondrial ROS detection. Data are expressed as mean ± SD (n = 12). ** $p < 0.01$ vs. Sham group; $^{\#\#}$ $p < 0.01$ vs. SCI + Oe-NC group. ROS, reactive oxygen species; DCFH-DA, 2′,7′-Dichlorodihydrofluorescein diacetate; CALM, calmodulin; MCU, mitochondrial calcium uniporter; JC-1, 5,5′,6,6′-Tetrachloro-1,1′,3,3′-tetraethylbenzimidazolylcarbocyanine iodide; RFU, relative fluorescence units.

TRPML1 group, exceeding Sham levels ($p < 0.01$), indicating the recovery of calcium-regulatory capacity. Consistently, total calcium levels in spinal cord tissues, which were elevated following SCI, were significantly reduced by TRPML1 overexpression (Fig. 2B), implying improved calcium homeostasis.

Oxidative stress, evaluated using DCFH-DA staining, revealed a substantial increase in ROS production after SCI, which was significantly attenuated by TRPML1 overexpression (Fig. 2C, $p < 0.01$). To assess mitochondrial function, JC-1 and MitoSOX assays were conducted to determine ΔΨm and mitochondrial ROS levels, respectively (Fig. 2D,E). SCI induced ΔΨm depolarization and mitochondrial ROS accumulation, both of which were effectively reversed with TRPML1 overexpression, indicating strong mitochondrial protective effects.

Collectively, these results demonstrate that TRPML1 overexpression alleviates calcium dysregulation, decreases oxidative stress, and maintains mitochondrial function after SCI, underscoring its significant neuroprotective potential.

Regulatory Role of TRPML1 in Apoptosis After SCI

To evaluate the effect of TRPML1 on apoptosis after SCI, TUNEL staining was performed (Fig. 3). Compared to the Sham group, the SCI group exhibited a significant increase in TUNEL-positive cells ($p < 0.01$), indicating enhanced neuronal apoptosis after injury. Conversely, TRPML1 overexpression substantially reduced the proportion of TUNEL-positive cells compared to both the SCI and Sham groups ($p < 0.01$). These findings suggest that TRPML1 overexpression mitigates SCI-induced apoptosis, supporting its potential neuroprotection role via anti-apoptotic mechanisms.

TRPML1 Ameliorates Histopathological Damage and Promotes Functional Recovery After SCI

To assess the impact of TRPML1 on spinal pathology and functional recovery after SCI, H&E staining and BMS scoring were conducted. As shown in Fig. 4A, the SCI group exhibited severe histopathological changes, including disorganized neuronal architecture, inflammatory cell infiltration, and extensive necrotic regions, compared to the Sham group. However, these abnormalities were markedly attenuated in the SCI + Oe-TRPML1 group, which showed a more organized tissue structure, reduced inflammation, and smaller necrotic areas. Furthermore, motor function, evaluated using the BMS (Fig. 4B), demonstrated a significant reduction in BMS scores in the SCI group on day 1

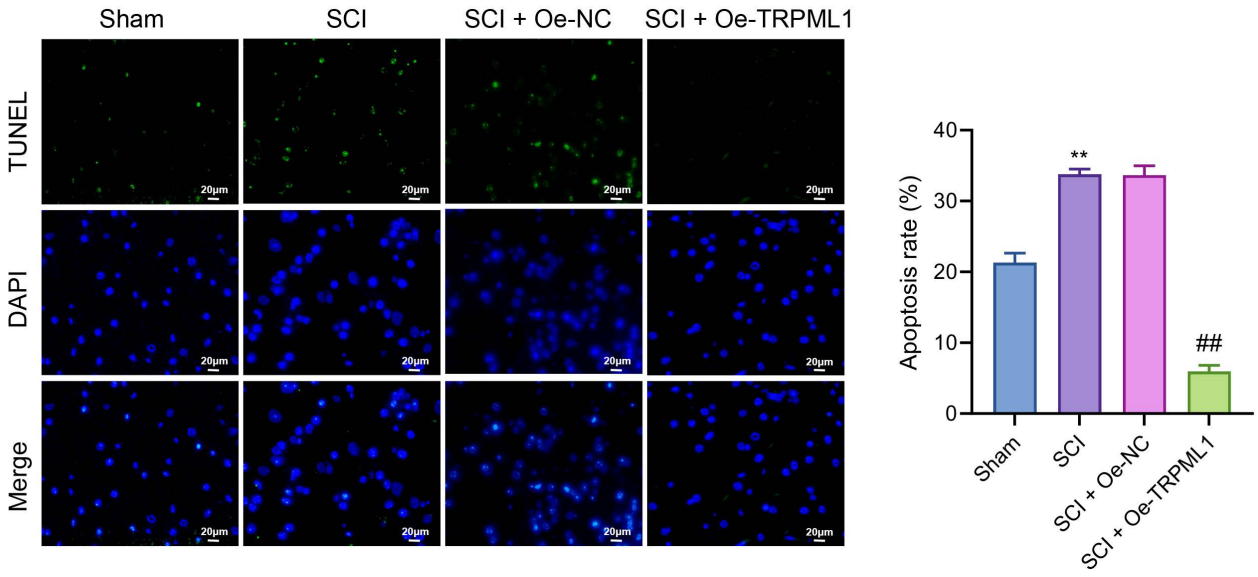

Fig. 3. Effects of TRPML1 on apoptosis after SCI. Representative TUNEL staining of spinal cord sections showing apoptotic cells (green) and nuclei (blue, DAPI). Scale bar: 20 μm. The right panel represents the quantification of the apoptotic rate across groups. Data are expressed as mean ± SD (n = 3). ** $p < 0.01$ vs. Sham group; $^{\#\#}$ $p < 0.01$ vs. SCI + Oe-NC group. TUNEL, terminal deoxynucleotidyl transferase dUTP nick end labeling; DAPI, 4′6-diamidino-2-phenylindole.

post-injury, with minimal improvement by day 3. From day 7 onward, all groups exhibited gradual recovery; however, the SCI + Oe-TRPML1 group achieved significantly higher BMS scores from days 7 to 28, with marked improvements in hindlimb coordination by day 14 and enhanced locomotor function at days 21 and 28 ($p < 0.01$). Although functional recovery in the SCI + Oe-TRPML1 group did not fully return to Sham levels by day 28, it was significantly greater than that of the SCI + Oe-NC groups ($p < 0.05$). These findings indicate that TRPML1 overexpression attenuates SCI-induced structural damage and facilitates sustained functional recovery.

TRPML1 Alleviates H_2O_2-Induced Injury in NSC-34 Cells by Regulating Mitochondrial/Lysosomal Proteins and Calcium Homeostasis

To further investigate the role of TRPML1 at the cellular level, an H_2O_2-induced injury model was established in NSC-34 cells, followed by TRPML1 overexpression. As shown in Fig. 5A,B, TRPML1 mRNA and protein expression levels were significantly elevated in the Oe-TRPML1 group compared to the Oe-NC group ($p < 0.01$), confirming successful overexpression. However, H_2O_2 treatment markedly suppressed TRPML1 mRNA expression, whereas exogenous overexpression effectively reversed this downregulation (Fig. 5C, $p < 0.01$), indicating that TRPML1 is sensitive to oxidative stress and can be restored via gene delivery.

Western blot analysis further demonstrated (Fig. 5D) that H_2O_2 exposure significantly reduced the expression of LAMP1, ATP5A1, and MCU compared to the control group, whereas overexpression of TRPML1 restored their levels ($p < 0.01$). These findings imply that TRPML1 may alleviate oxidative stress-induced cellular damage by modulating proteins associated with mitochondrial and lysosomal function. Moreover, H_2O_2 treatment significantly increased intracellular Ca^{2+} concentration, while TRPML1 overexpression substantially reduced this Ca^{2+} overload (Fig. 5E, $p < 0.01$), underscoring its role in maintaining calcium homeostasis under stress conditions.

TRPML1 Attenuates ROS Accumulation, Mitochondrial Dysfunction, and H_2O_2-Induced Apoptosis in NSC-34 Cells

To further verify the protective role of TRPML1 in the H_2O_2-induced injury model, intracellular ROS levels, $\Delta\Psi m$, and apoptosis rate were evaluated in NSC-34 cells. As shown in Fig. 6A, H_2O_2 exposure significantly increased intracellular ROS accumulation, whereas TRPML1 overexpression effectively suppressed ROS levels ($p < 0.01$), suggesting its antioxidative potential. Furthermore, TUNEL staining (Fig. 6B) demonstrated a significant increase in apoptosis rates following H_2O_2 treatment, whereas TRPML1 overexpression significantly reduced the proportion of TUNEL-positive cells ($p < 0.01$), indicating its cytoprotective role under oxidative stress.

Moreover, JC-1 staining (Fig. 6C) revealed that H_2O_2 significantly reduced $\Delta\Psi m$, which was effectively restored by TRPML1 overexpression ($p < 0.01$), suggesting its potential for mitochondrial protection. Collectively, these re-

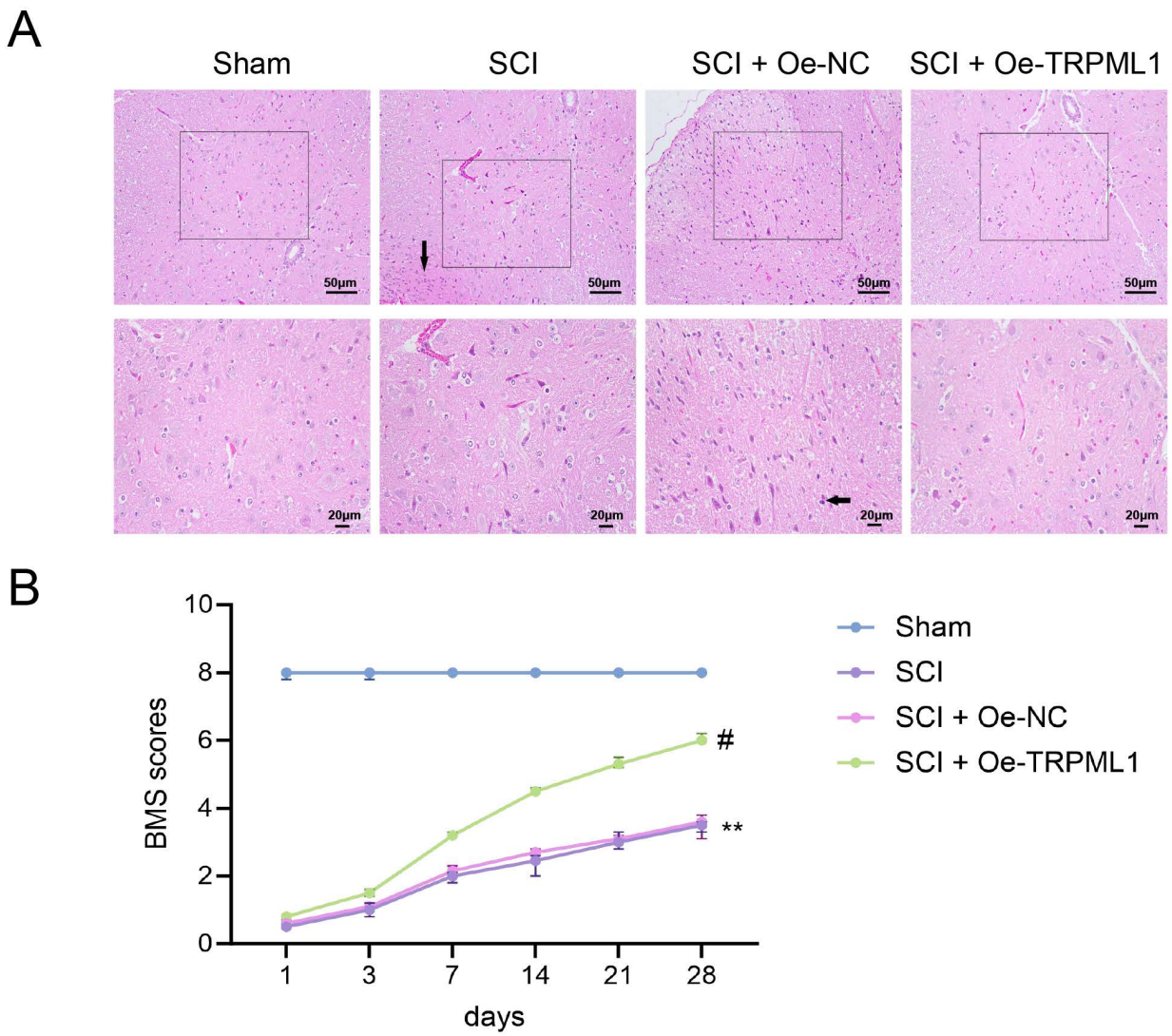

Fig. 4. TRPML1 overexpression improves histopathological outcomes and promotes motor function recovery after SCI. (A) H&E staining of spinal cord tissue in different experimental groups. Black arrows indicate areas of neuronal disorganization and severe tissue necrosis. TRPML1 overexpression reduced inflammatory infiltration and tissue damage. Scale bar = 50 μm (top), 20 μm (bottom). (B) BMS scores were recorded on days 1, 3, 7, 14, 21, and 28 post-injuries to assess locomotor recovery. Data are expressed as mean ± SD (n = 12). ** $p < 0.01$ vs. Sham group; $^{\#}$ $p < 0.05$ vs. SCI + Oe-NC group. BMS, basso mouse scale; H&E, hematoxylin and eosin.

sults demonstrate that TRPML1 alleviates oxidative stress-induced cellular dysfunction by attenuating ROS accumulation, preserving mitochondrial integrity, and inhibiting apoptosis.

Discussion

This study comprehensively investigated the role and molecular mechanisms of TRPML1 in SCI repair, demonstrating that TRPML1 overexpression confers significant neuroprotective effects both *in vivo* and *in vitro*. In the SCI mouse model, TRPML1 expression was significantly downregulated following injury, accompanied by cellular calcium overload, elevated oxidative stress, a decline in $\Delta\Psi m$, and increased neuronal apoptosis. TRPML1 overexpression reversed these pathological changes by upregulating key regulatory proteins, such as CALM, MCU, TFEB, LAMP1, and ATP5A1, thereby restoring calcium homeostasis, enhancing lysosomal and mitochondrial function, and reducing Cytochrome C release and alleviating ROS accumulation. These molecular and cellular improvements were reflected by attenuated neuronal apoptosis, improved tissue morphology, and enhanced motor performance. Moreover, similar protective effects were observed in the H_2O_2-induced NSC-34 cell injury model. These findings collectively underscore the role of TRPML1 as a key modulator of neuroprotection in the context of SCI.

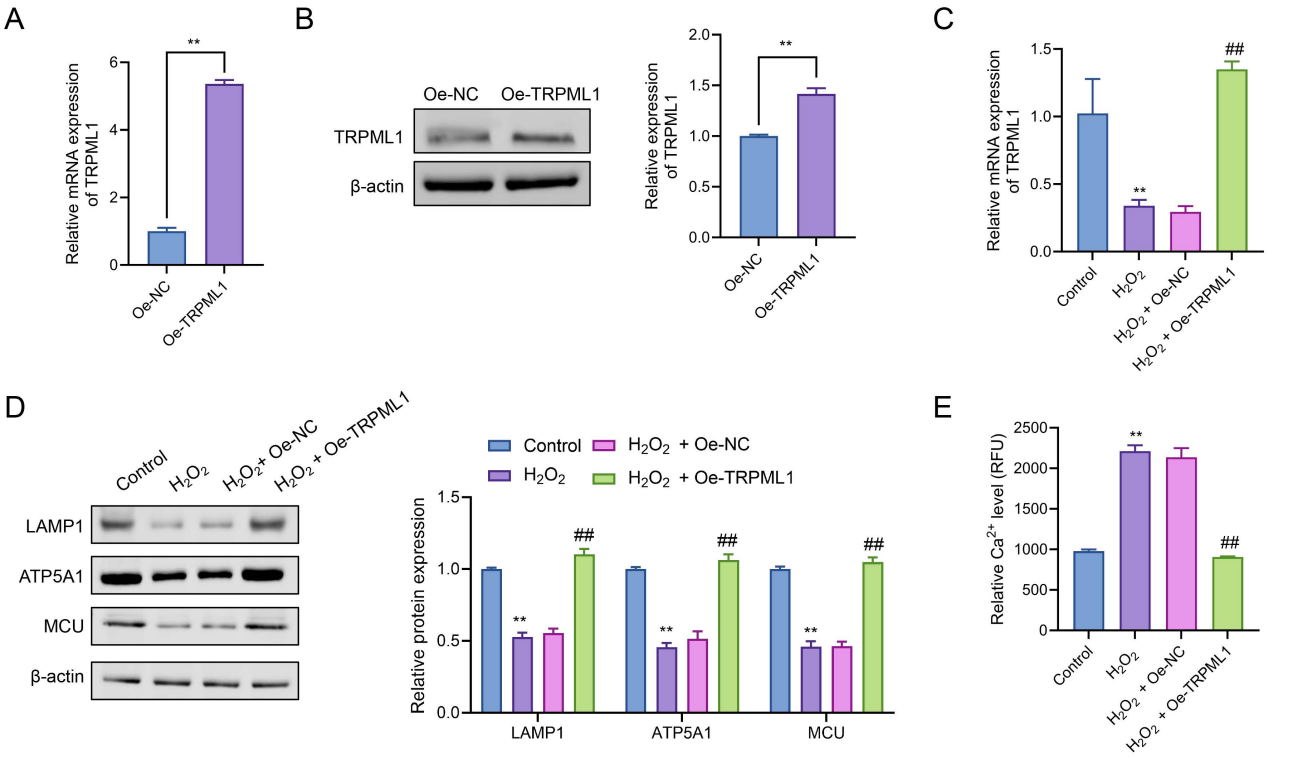

Fig. 5. TRPML1 regulates mitochondrial and lysosomal protein expression and calcium homeostasis in NSC-34 cells under H_2O_2-induced oxidative stress. (A,B) TRPML1 mRNA and protein expression levels in Oe-NC and Oe-TRPML1 groups. (C) qRT-PCR analysis of TRPML1 mRNA in different treatment groups. (D) Western blot analysis and quantification of LAMP1, ATP5A1, and MCU protein levels. (E) Intracellular Ca^{2+} levels. Data are expressed as mean ± SD (n = 3). ** $p < 0.01$ vs. Control group; $^{\#\#}$ $p < 0.01$ vs. H_2O_2 + Oe-NC group. H_2O_2, hydrogen peroxide.

These results are consistent with previous studies that have identified TRPML1 as a critical regulator of lysosomal calcium channels, lysosome–mitochondria communication, and intracellular homeostasis [32,33]. SCI-induced secondary damage is known to disrupt lysosomal calcium flux and impair mitochondrial function [34,35]. Our findings demonstrate that TRPML1 overexpression upregulates the expression of CALM and MCU proteins, reduces calcium ion accumulation, and improves mitochondrial function. Additionally, while SCI increases ROS levels, leading to mitochondrial damage and oxidative stress [36], TRPML1 overexpression was observed to enhance lysosomal biogenesis via the TFEB signaling pathway, improve mitochondrial autophagy, and reduce oxidative stress.

Previous studies have shown that SCI-induced lysosomal dysfunction impairs the clearance of damaged organelles, leading to neuronal death [1,37], whereas activation of TRPML1 promotes mitochondrial autophagy and reduces SCI-associated apoptosis [19]. This study further confirms the protective role of TRPML1 in SCI repair, demonstrating that its overexpression reduces Cytochrome C release and inhibits the mitochondria-dependent apoptosis pathway [38,39]. Moreover, AAV-mediated TRPML1 overexpression has been shown to enhance motor function recovery and promote neuroregeneration [40], findings that align with the improved BMS score found in this study. Notably, similar to recent reports demonstrating early functional improvements with AAV-mediated gene therapy in spinal cord injury models [41], the neuroprotection observed as early as 7 days post-injury in this study may indicate rapid transcriptional responses induced by viral transduction before peak transgene expression. Collectively, these results underscore TRPML1 as a promising therapeutic target for managing SCI.

The *in vitro* mechanistic studies further corroborated these findings. In the H_2O_2-induced NSC-34 motor neuron injury model, TRPML1 overexpression significantly restored calcium homeostasis, reduced ROS levels, improved $\Delta\Psi m$, and suppressed apoptosis. These protective effects are likely driven by enhanced lysosome–mitochondria coupling, facilitated autophagic clearance of damaged organelles, and improved cellular energy metabolism [22]. Notably, these *in vitro* results closely aligned with the *in vivo* observations, collectively indicating that TRPML1 confers neuroprotection in SCI by modulating calcium signaling and maintaining mitochondrial stability.

Despite revealing the neuroprotective mechanisms of TRPML1 in SCI repair, this study has certain limitations.

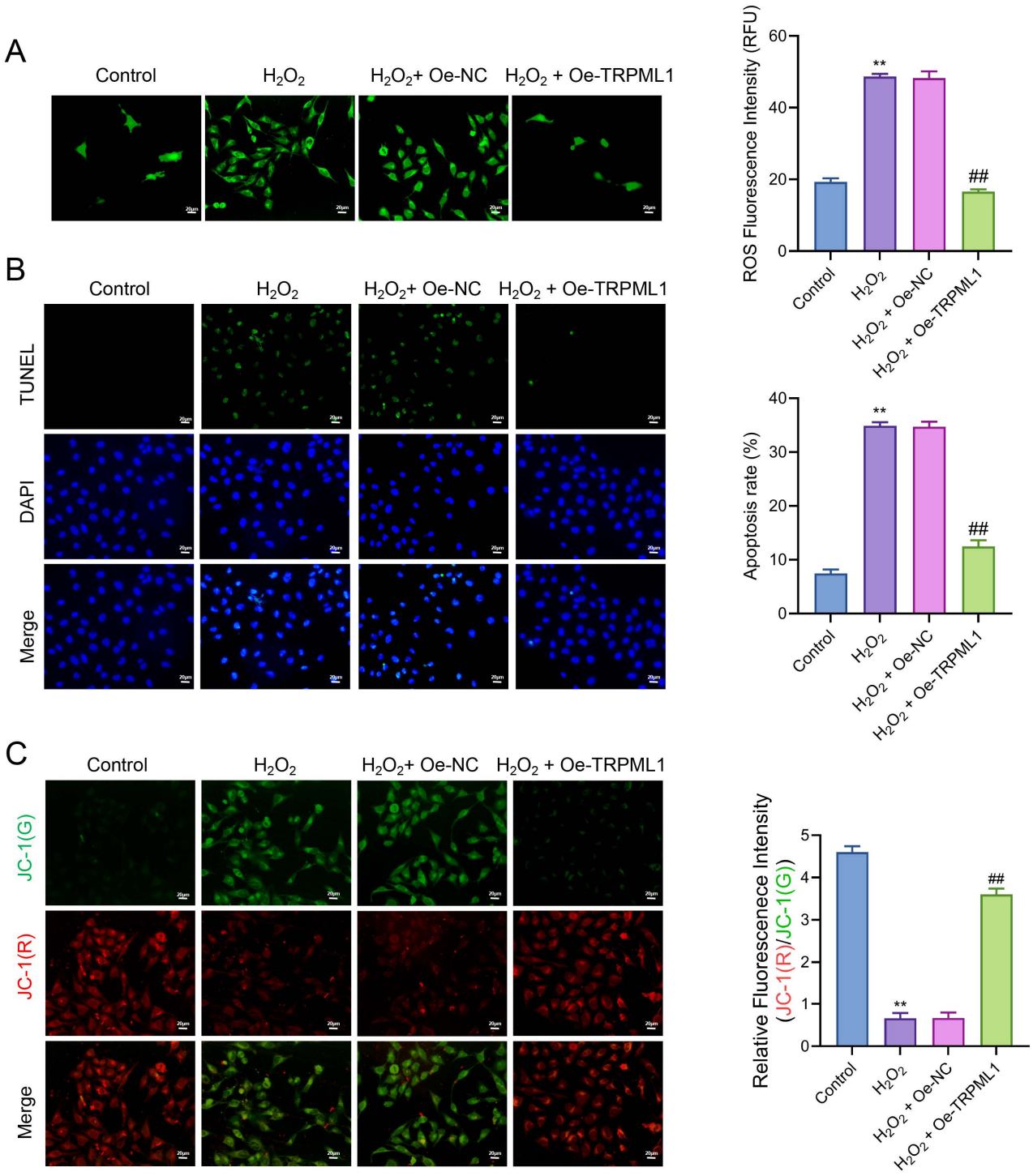

Fig. 6. TRPML1 overexpression attenuates H_2O_2-induced cellular dysfunction in NSC-34 cells. (A) Intracellular ROS levels were determined using DCFH-DA staining. (B) Apoptotic cell proportion detected using TUNEL staining. (C) Mitochondrial membrane potential assessed using JC-1 staining (red/green fluorescence). Data are expressed as mean ± SD (n = 3). ** $p < 0.01$ vs. Control group; $^{\#\#}$ $p < 0.01$ vs. H_2O_2 + Oe-NC group.

First, although AAV9 vectors with the CamKII promoter were used to enhance neuronal targeting, neuronal specificity and lysosomal localization of TRPML1 were not directly validated *in vivo* or *in vitro* (e.g., via co-staining with NeuN or LAMP1), which may affect the interpretation of cell-type-specific effects. Second, the temporal dynamics of AAV9-mediated expression were not evaluated, making it unclear whether early-stage improvements were directly attributable to TRPML1 activity. Third, the relatively small sample size in molecular experiments may have lim-

ited statistical power despite clear trends. Fourth, although TUNEL staining confirmed reduced apoptosis, the specific cell type undergoing apoptosis was not identified due to the absence of neuronal or glial markers. Fifth, although ROS, Ca^{2+}, and mitochondrial potential were assessed using widely accepted fluorescent probes, the lack of positive or negative controls (e.g., NAC, BAPTA-AM, CCCP) may limit signal specificity. Lastly, this study used only a murine model and primarily focused on motor outcomes. Future studies should incorporate time-course validation of expression, lineage tracing, pharmacological controls, and larger sample sizes to strengthen mechanistic insight and translational applicability.

In summary, TRPML1 exerts multi-faceted neuroprotective effects in SCI repair by modulating calcium signaling, enhancing lysosome–mitochondria coordination, suppressing oxidative stress, and inhibiting apoptosis. These findings not only expand our understanding of TRPML1's role in secondary injury mechanisms but also underscore its potential as a promising therapeutic target for gene- and pharmacological-based interventions.

Conclusion

This study reveals that TRPML1 plays a pivotal role in SCI repair. Its overexpression restores calcium signaling, improves lysosome-mitochondria interactions, attenuates oxidative stress, and suppresses apoptosis, thereby facilitating tissue preservation and recovery of motor function. These findings highlight TRPML1 as a promising therapeutic target for managing SCI, providing a basis for future investigations into its clinical applications.

Availability of Data and Materials

The datasets used and analyzed during the current study are available from the corresponding author on reasonable request.

Author Contributions

JLZ: Conceptualization, Formal analysis, Writing — Original draft and Writing — Review and Editing; JK: Methodology, Data curation, Writing — Original draft and Writing — Review and Editing; ZYZ: Formal analysis and Writing — Review and Editing; HZ: Formal analysis and Writing — Review and Editing; RBB: Data curation and Writing — Review and Editing; SY: Methodology, Writing — Review and Editing, Funding acquisition and Supervision. All authors have given final approval of the version to be published; have agreed on the journal to which the article has been submitted; and have agreed to be accountable for all aspects of the work.

Ethics Approval and Consent to Participate

All animal protocols were approved by the Animal Ethics Committee of the Guangdong Provincial Medical Laboratory Animal Center, China (Approval No. D202504-11) and conducted in accordance with institutional and national guidelines for animal research.

Acknowledgment

Not applicable.

Funding

This study is supported by Natural Science Foundation of Gansu Province (No. 24JRRA1109).

Conflict of Interest

The authors declare no conflict of interest.

Supplementary Material

Supplementary material associated with this article can be found, in the online version, at https://doi.org/10.24976/Discov.Med.202537201.192.

References

[1] Bisicchia E, Mastrantonio R, Nobili A, Palazzo C, La Barbera L, Latini L, *et al*. Restoration of ER proteostasis attenuates remote apoptotic cell death after spinal cord injury by reducing autophagosome overload. Cell Death & Disease. 2022; 13: 381. https://doi.org/10.1038/s41419-022-04830-9.

[2] Li Y, Jones JW, M C Choi H, Sarkar C, Kane MA, Koh EY, *et al*. cPLA2 activation contributes to lysosomal defects leading to impairment of autophagy after spinal cord injury. Cell Death & Disease. 2019; 10: 531. https://doi.org/10.1038/s41419-019-1764-1.

[3] Tedeschi V, Petrozziello T, Secondo A. Calcium Dyshomeostasis and Lysosomal Ca^{2+} Dysfunction in Amyotrophic Lateral Sclerosis. Cells. 2019; 8: 1216. https://doi.org/10.3390/cells8101216.

[4] GBD Spinal Cord Injuries Collaborators. Global, regional, and national burden of spinal cord injury, 1990-2019: a systematic analysis for the Global Burden of Disease Study 2019. The Lancet Neurology. 2023; 22: 1026–1047. https://doi.org/10.1016/S1474-4422(23)00287-9.

[5] McDonald JW, Sadowsky C. Spinal-cord injury. Lancet (London, England). 2002; 359: 417–425. https://doi.org/10.1016/S0140-6736(02)07603-1.

[6] Guha L, Singh N, Kumar H. Different Ways to Die: Cell Death Pathways and Their Association With Spinal Cord Injury. Neurospine. 2023; 20: 430–448. https://doi.org/10.14245/ns.2244976.488.

[7] Whittemore SR, Saraswat Ohri S, Forston MD, Wei GZ, Hetman M. The Proteostasis Network: A Global Therapeutic Target for Neuroprotection after Spinal Cord Injury. Cells. 2022; 11: 3339. https://doi.org/10.3390/cells11213339.

[8] Zhang J, Tang Y, Hu Z, Xu W, Ma Y, Xu P, *et al*. The inhibition of TRPML1/TFEB leads to lysosomal biogenesis disorder, contributes to developmental fluoride neurotoxicity. Eco-

toxicology and Environmental Safety. 2023; 250: 114511. https://doi.org/10.1016/j.ecoenv.2023.114511.

[9] Hou M, Zhang Z, Fan Z, Huang L, Wang L. The mechanisms of Ca2+ regulating autophagy and its research progress in neurodegenerative diseases: A review. Medicine. 2024; 103: e39405. https://doi.org/10.1097/MD.0000000000039405.

[10] Gorgey AS, Witt O, O'Brien L, Cardozo C, Chen Q, Lesnefsky EJ, *et al*. Mitochondrial health and muscle plasticity after spinal cord injury. European Journal of Applied Physiology. 2019; 119: 315–331. https://doi.org/10.1007/s00421-018-4039-0.

[11] Perrone M, Patergnani S, Di Mambro T, Palumbo L, Wieckowski MR, Giorgi C, *et al*. Calcium Homeostasis in the Control of Mitophagy. Antioxidants & Redox Signaling. 2023; 38: 581–598. https://doi.org/10.1089/ars.2022.0122.

[12] Cheng L, Cai B, Lu D, Zeng H. The role of mitochondrial energy metabolism in neuroprotection and axonal regeneration after spinal cord injury. Mitochondrion. 2023; 69: 57–63. https://doi.org/10.1016/j.mito.2023.01.009.

[13] He Z, Du J, Zhang Y, Xu Y, Huang Q, Zhou Q, *et al*. Kruppel-like factor 2 contributes to blood-spinal cord barrier integrity and functional recovery from spinal cord injury by augmenting autophagic flux. Theranostics. 2023; 13: 849–866. https://doi.org/10.7150/thno.74324.

[14] Springer JE, Azbill RD, Knapp PE. Activation of the caspase-3 apoptotic cascade in traumatic spinal cord injury. Nature Medicine. 1999; 5: 943–946. https://doi.org/10.1038/11387.

[15] Galluzzi L, Bravo-San Pedro JM, Blomgren K, Kroemer G. Autophagy in acute brain injury. Nature Reviews. Neuroscience. 2016; 17: 467–484. https://doi.org/10.1038/nrn.2016.51.

[16] Chen L, Liu H, Jiang L, Wang Z, Chang Y, Li N, *et al*. Lipid Droplets Metabolism Mediated by ANXA7-PPARγ Signaling Axis Regulates Spinal Cord Injury Repair in Mice. Advanced Science (Weinheim, Baden-Wurttemberg, Germany). 2025; 12: e2417326. https://doi.org/10.1002/advs.202417326.

[17] Pedroni A, Dai YWE, Lafouasse L, Chang W, Srivastava I, Del Vecchio L, *et al*. Neuroprotective gap-junction-mediated bystander transformations in the adult zebrafish spinal cord after injury. Nature Communications. 2024; 15: 4331. https://doi.org/10.1038/s41467-024-48729-9.

[18] Peng T, Xie Y, Zhao S, Wang X, Zhang W, Xie Y, *et al*. TRPML1 ameliorates seizures-related neuronal injury by regulating autophagy and lysosomal biogenesis via Ca^{2+}/TFEB signaling pathway. Biochimica et Biophysica Acta. Molecular Basis of Disease. 2024; 1870: 167477. https://doi.org/10.1016/j.bbadis.2024.167477.

[19] Lou J, Jin M, Zhou C, Fan Y, Ni L, Mao Y, *et al*. Ezrin inhibition alleviates oxidative stress and pyroptosis via regulating TRPML1-calcineurin axis mediated enhancement of autophagy in spinal cord injury. Free Radical Biology & Medicine. 2024; 212: 133–148. https://doi.org/10.1016/j.freeradbiomed.2023.12.020.

[20] Liu P, Liu X, Wu Z, Shen K, Li Z, Li X, *et al*. Size effect-based improved antioxidant activity of selenium nanoparticles regulating Anti-PI3K-mTOR and Ras-MEK pathways for treating spinal cord injury to avoid hormone shock-induced immunosuppression. Journal of Nanobiotechnology. 2025; 23: 17. https://doi.org/10.1186/s12951-024-03054-7.

[21] Feng X, Cai W, Li Q, Zhao L, Meng Y, Xu H. Activation of lysosomal Ca2+ channels mitigates mitochondrial damage and oxidative stress. The Journal of Cell Biology. 2025; 224: e202403104. https://doi.org/10.1083/jcb.202403104.

[22] Peng W, Wong YC, Krainc D. Mitochondria-lysosome contacts regulate mitochondrial Ca^{2+} dynamics via lysosomal TRPML1. Proceedings of the National Academy of Sciences of the United States of America. 2020; 117: 19266–19275. https://doi.org/10.1073/pnas.2003236117.

[23] Xiang L, Lou J, Zhao J, Geng Y, Zhang J, Wu Y, *et al*. Underlying Mechanism of Lysosomal Membrane Permeabilization in CNS Injury: A Literature Review. Molecular Neurobiology. 2025; 62: 626–642. https://doi.org/10.1007/s12035-024-04290-6.

[24] Zhang H, Wang W, Hu X, Wang Z, Lou J, Cui P, *et al*. Heterophyllin B enhances transcription factor EB-mediated autophagy and alleviates pyroptosis and oxidative stress after spinal cord injury. International Journal of Biological Sciences. 2024; 20: 5415–5435. https://doi.org/10.7150/ijbs.97669.

[25] Wang H, Zhu Y, Liu H, Liang T, Wei Y. Advances in Drug Discovery Targeting Lysosomal Membrane Proteins. Pharmaceuticals (Basel, Switzerland). 2023; 16: 601. https://doi.org/10.3390/ph16040601.

[26] Santoni G, Maggi F, Amantini C, Marinelli O, Nabissi M, Morelli MB. Pathophysiological Role of Transient Receptor Potential Mucolipin Channel 1 in Calcium-Mediated Stress-Induced Neurodegenerative Diseases. Frontiers in Physiology. 2020; 11: 251. https://doi.org/10.3389/fphys.2020.00251.

[27] Barral DC, Staiano L, Guimas Almeida C, Cutler DF, Eden ER, Futter CE, *et al*. Current methods to analyze lysosome morphology, positioning, motility and function. Traffic (Copenhagen, Denmark). 2022; 23: 238–269. https://doi.org/10.1111/tra.12839.

[28] Sapienza S, Tedeschi V, Apicella B, Palestra F, Russo C, Piccialli I, *et al*. Size-Based Effects of Anthropogenic Ultrafine Particles on Lysosomal TRPML1 Channel and Autophagy in Motoneuron-like Cells. International Journal of Molecular Sciences. 2022; 23: 13041. https://doi.org/10.3390/ijms232113041.

[29] Hook MA, Falck A, Dundumulla R, Terminel M, Cunningham R, Sefiani A, *et al*. Osteopenia in a Mouse Model of Spinal Cord Injury: Effects of Age, Sex and Motor Function. Biology. 2022; 11: 189. https://doi.org/10.3390/biology11020189.

[30] Basso DM, Fisher LC, Anderson AJ, Jakeman LB, McTigue DM, Popovich PG. Basso Mouse Scale for locomotion detects differences in recovery after spinal cord injury in five common mouse strains. Journal of Neurotrauma. 2006; 23: 635–659. https://doi.org/10.1089/neu.2006.23.635.

[31] Jia CJ, Chen MN, Huang DD, Wu SF, Zeng CM, Liu ZQ, *et al*. Edaravone promotes motoneuron survival and functional recovery after brachial plexus root avulsion and reimplantation in rats: Involvement of SIRT1/TFEB pathway. International Immunopharmacology. 2025; 145: 113686. https://doi.org/10.1016/j.intimp.2024.113686.

[32] Kendall RL, Holian A. The role of lysosomal ion channels in lysosome dysfunction. Inhalation Toxicology. 2021; 33: 41–54. https://doi.org/10.1080/08958378.2021.1876188.

[33] Qi J, Li Q, Xin T, Lu Q, Lin J, Zhang Y, *et al*. MCOLN1/TRPML1 in the lysosome: a promising target for autophagy modulation in diverse diseases. Autophagy. 2024; 20: 1712–1722. https://doi.org/10.1080/15548627.2024.2333715.

[34] Dumont RJ, Okonkwo DO, Verma S, Hurlbert RJ, Boulos PT, Ellegala DB, *et al*. Acute spinal cord injury, part I: pathophysiologic mechanisms. Clinical Neuropharmacology. 2001; 24: 254–264. https://doi.org/10.1097/00002826-200109000-00002.

[35] Liu S, Li Y, Choi HMC, Sarkar C, Koh EY, Wu J, *et al*. Lysosomal damage after spinal cord injury causes accumulation of RIPK1 and RIPK3 proteins and potentiation of necroptosis. Cell Death & Disease. 2018; 9: 476. https://doi.org/10.1038/s41419-018-0469-1.

[36] Liu C, Hu F, Jiao G, Guo Y, Zhou P, Zhang Y, *et al*. Dental pulp stem cell-derived exosomes suppress M1 macrophage polarization through the ROS-MAPK-NFκB P65 signaling pathway after spinal cord injury. Journal of Nanobiotechnology. 2022; 20: 65. https://doi.org/10.1186/s12951-022-01273-4.

[37] Liu S, Sarkar C, Dinizo M, Faden AI, Koh EY, Lipinski MM, *et al*. Disrupted autophagy after spinal cord injury is associated

with ER stress and neuronal cell death. Cell Death & Disease. 2015; 6: e1582. https://doi.org/10.1038/cddis.2014.527.

[38] Kondratskyi A, Kondratska K, Skryma R, Prevarskaya N. Ion channels in the regulation of apoptosis. Biochimica et Biophysica Acta. 2015; 1848: 2532–2546. https://doi.org/10.1016/j.bbamem.2014.10.030.

[39] Cheng X, Shen D, Samie M, Xu H. Mucolipins: Intracellular TRPML1-3 channels. FEBS Letters. 2010; 584: 2013–2021. https://doi.org/10.1016/j.febslet.2009.12.056.

[40] Sangster M, Shahriar S, Niziolek Z, Carisi MC, Lewandowski M, Budnik B, *et al*. Brain cell type specific proteomics approach to discover pathological mechanisms in the childhood CNS disorder mucolipidosis type IV. Frontiers in Molecular Neuroscience. 2023; 16: 1215425. https://doi.org/10.3389/fnmol.2023.1215425.

[41] Chen Y, Wu L, Shi M, Zeng D, Hu R, Wu X, *et al*. Electroacupuncture Inhibits NLRP3 Activation by Regulating CMPK2 After Spinal Cord Injury. Frontiers in Immunology. 2022; 13: 788556. https://doi.org/10.3389/fimmu.2022.788556.